中山大學
SUN YAT-SEN UNIVERSITY

Studying the $b \to s\ell^+\ell^-$ Anomalies and $(g-2)_\mu$ in RPV-MSSM Framework with Inverse Seesaw

Min-Di Zheng

11/11/2021

In collaboration with Hong-Hao Zhang

HFCPV 2021, JNU

Outlines

- Motivation
- Model: RPV-MSSMIS
- $b \to s\ell^+\ell^-$ process
- $(g-2)_\mu$ and constraints
- Numerical discussions and conclusions

R_K

$$R_K = \frac{\Gamma(B \to K \mu^+ \mu^-)}{\Gamma(B \to K e^+ e^-)}$$

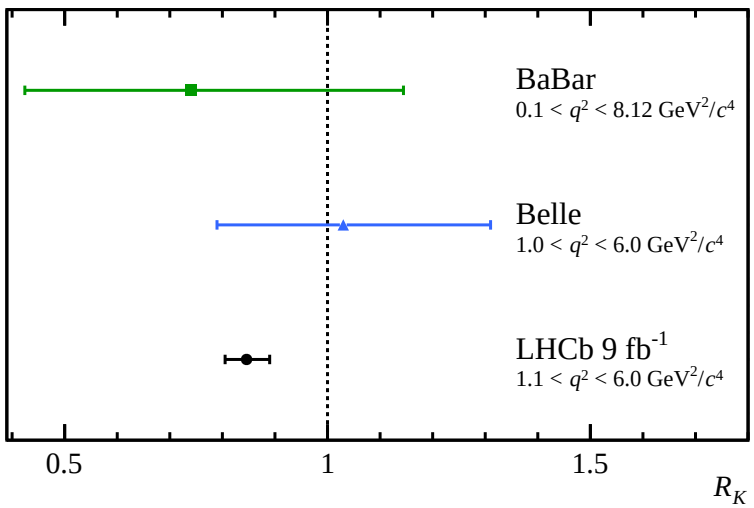

$R_K^{\rm exp}$ by LHCb (q^2 bin $[1.1, 6]$ GeV^2)

PRL 122 (2019) 19, 191801:

$$R_K^{\rm (previous)} = 0.846^{+0.060\ +0.016}_{-0.054\ -0.014},$$

deviates from SM by 2.5σ

2103.11769:

$$R_K^{\rm (full\ run\ II)} = 0.846^{+0.042\ +0.013}_{-0.039\ -0.012},$$

deviates from SM by 3.1σ

indicate NP that breaks lepton flavour universality (LFU)

R_{K^*}

$$R_{K^*} = \frac{\Gamma(B \to K^* \mu^+ \mu^-)}{\Gamma(B \to K^* e^+ e^-)}$$

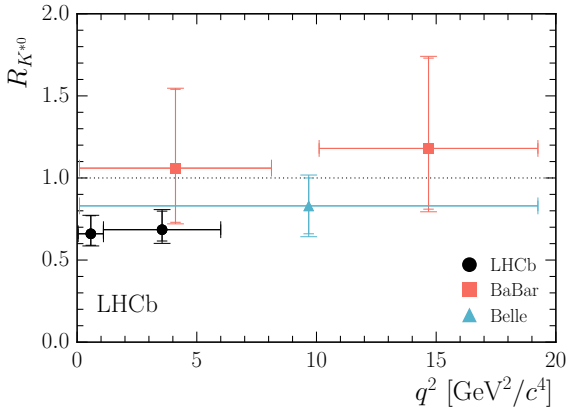

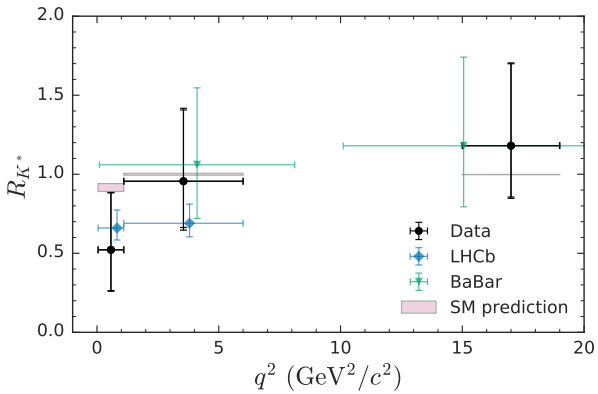

M. Bordone *et al.*, EPJC 76 (2016) 8, 440

$$R_{K^*}^{\rm SM} = \begin{cases} 0.906 \pm 0.028, & 0.045 < q^2 < 1.1 \text{ GeV}^2 \\ 1.00 \pm 0.01, & 1.1 < q^2 < 6.0 \text{ GeV}^2 \end{cases}$$

LHCb, JHEP 08 (2017) 055

$$R_{K^*}^{\rm LHCb} = \begin{cases} 0.66^{+0.11}_{-0.07} \pm 0.03, & 0.045 < q^2 < 1.1 \text{ GeV}^2 \\ 0.69^{+0.11}_{-0.07} \pm 0.05, & 1.1 < q^2 < 6.0 \text{ GeV}^2 \end{cases}$$

deviate from SM by $(2.1)2.5\sigma$ respectively

The model-independent global fit

$$\mathcal{L}_{\text{eff}} = \frac{4G_F}{\sqrt{2}} K_{tb}K_{ts}^* \sum_i C_i \mathcal{O}_i + \text{h.c.}$$

$$\mathcal{O}_9 = \frac{e^2}{16\pi^2}(\bar{s}\gamma_\mu P_L b)(\bar{\ell}\gamma^\mu \ell), \quad \mathcal{O}_{10} = \frac{e^2}{16\pi^2}(\bar{s}\gamma_\mu P_L b)(\bar{\ell}\gamma^\mu \gamma_5 \ell)$$

$$\begin{aligned} C_{9,\mu}^{\text{NP}} &= C_{\text{V}} + C_{\text{U}}, \quad C_{10,\mu}^{\text{NP}} = -C_{\text{V}} \\ C_{9,e}^{\text{NP}} &= C_{\text{U}}, \quad C_{10,e}^{\text{NP}} = 0 \end{aligned}$$

Scenario A: $C_{\text{U}} = 0 \;\Rightarrow\; C_{9,\mu}^{\text{NP}} = -C_{10,\mu}^{\text{NP}}$

Scenario B: $C_{\text{U}} \neq 0$

Fit results adopted

W. Altmannshofer and P. Stangl, EPJC 81 (2021) 10, 952

Scenario A (1σ):

Wilson coefficients	$b \to s\mu^+\mu^-$ ($\mathcal{B}$ and angular)	$R_{K^{(*)}}$, $D_{P'_{4,5}}$ and $B_s \to \mu^+\mu^-$	Combined results
$C_{9,\mu}^{\rm NP} = -C_{10,\mu}^{\rm NP} = C_{\rm V}$	$-0.53^{+0.13}_{-0.13}$	$-0.35^{+0.08}_{-0.08}$	$-0.39^{+0.07}_{-0.07}$

Scenario B(1σ to 2σ):

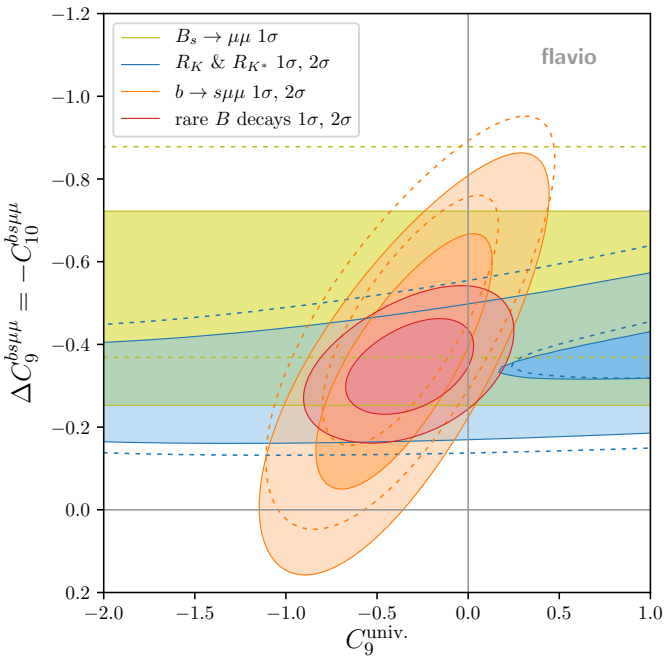

the new angular analyses of $B^0 \to K^{*0}\mu^+\mu^-$

LHCb, PRL 125 (2020) 1, 011802

and $B^\pm \to K^{*\pm}\mu^+\mu^-$

LHCb, PRL 126 (2021) 16, 161802

the updated branching ratio of the $B_s \to \phi\mu^+\mu^-$

LHCb, PRL 127 (2021) 15, 151801

$B_s \to \mu^+\mu^-$

CMS, JHEP 04 (2020) 188

LHCb, 2108.09283, 2108.09284

where $C_9^{\rm univ.} = C_{\rm U}$ and $\Delta C_9^{bs\mu\mu} = C_{\rm V}$

$(g-2)_\mu$

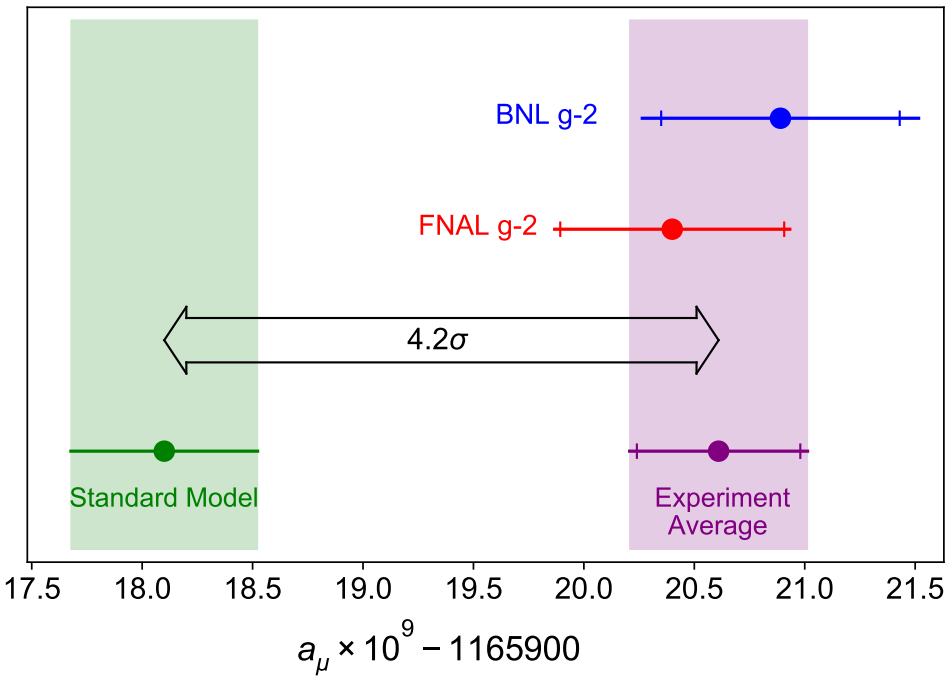

T. Aoyama *et al.* Phys.Rept. 887 (2020)

$$a_\mu^{\rm SM} = 116\ 591\ 810(43) \times 10^{-11}$$

B. Abi *et al.* PRL 126 (2021) 14, 141801

$$a_\mu^{\rm exp} = 116\ 592\ 061(41) \times 10^{-11}$$

$$\Delta a_\mu = a_\mu^{\rm exp} - a_\mu^{\rm SM} = (2.51 \pm 0.59) \times 10^{-9}$$

deviate from SM by 4.2σ!

Recent lattice QCD calculation

$a_\mu^{\rm LO-HVP} = 707.5(5.5) \times 10^{-10}$

(S. Borsanyi *et al.*, Nature 593 (2021) 7857)

weakens the tension, but has deviations with R-ratio results.

G. Colangelo *et al.*, JHEP 02 (2019) 006,
M. Davier *et al.*, EPJC 80 (2020) 3, 241,
A. Keshavarzi *et al.*, PRD 101 (2020) 1, 014029,
M. Hoferichter *et al.*, JHEP 08 (2019) 137

Even the large HVP contribution can account for the measurement of a_μ, there exists the tension within the electroweak fit.

A. Crivellin *et al.*, PRL 125 (2020) 9, 091801
A. Keshavarzi *et al.*, PRD 102 (2020) 3, 033002

E. de Rafael, PRD 102 (2020) 5, 056025

RPV-MSSMIS

The superpotential:

$$\mathcal{W} = \mathcal{W}_{\rm MSSM} + Y_\nu^{ij}\hat{R}_i\hat{L}_j\hat{H}_u + M_R^{ij}\hat{R}_i\hat{S}_j + \frac{1}{2}\mu_S^{ij}\hat{S}_i\hat{S}_j + \lambda'_{ijk}\hat{L}_i\hat{Q}_j\hat{D}_k,$$
$$\mathcal{W}_{\rm MSSM} = \mu\hat{H}_u\hat{H}_d + Y_u^{ij}\hat{U}_i\hat{Q}_j\hat{H}_u - Y_d^{ij}\hat{D}_i\hat{Q}_j\hat{H}_d - Y_e^{ij}\hat{E}_i\hat{L}_j\hat{H}_d$$

The soft SUSY breaking terms:

$$\begin{aligned}-\mathcal{L}^{\rm soft} =& -\mathcal{L}^{\rm soft}_{\rm MSSM} + (m^2_{\tilde{R}})_{ij}\tilde{R}_i^*\tilde{R}_j + (m^2_{\tilde{S}})_{ij}\tilde{S}_i^*\tilde{S}_j \\ &+ (A_\nu Y_\nu)_{ij}\tilde{R}_i^*\tilde{L}_j H_u + B^{ij}_{M_R}\tilde{R}_i^*\tilde{S}_j + \frac{1}{2}B^{ij}_{\mu_S}\tilde{S}_i\tilde{S}_j\end{aligned}$$

In the (ν, R, S) basis,

$$\mathcal{M}_\nu = \begin{pmatrix} 0 & m_D^T(=\frac{1}{\sqrt{2}}v_u Y_\nu) & 0 \\ m_D & 0 & M_R \\ 0 & M_R^T & \mu_S \end{pmatrix} = \mathcal{V}^\dagger \begin{pmatrix} m_{\nu_l}^{\rm diag} & 0 \\ 0 & m_{\nu_h}^{\rm diag} \end{pmatrix} \mathcal{V}^*$$
$$\Rightarrow \mu_S = (m_D^T)^{-1} M_R U_{\rm PMNS} m_\nu^{\rm diag} U_{\rm PMNS}^T M_R^T m_D^{-1}, \quad \text{when} \quad \mu_S \ll m_D < M_R$$

RPV-MSSMIS

In the $(\tilde{\nu}_L^{\mathcal{I}(\mathcal{R})}, \tilde{R}^{\mathcal{I}(\mathcal{R})}, \tilde{S}^{\mathcal{I}(\mathcal{R})})$ basis,

$$\mathcal{M}^2_{\tilde{\nu}^{\mathcal{I}(\mathcal{R})}} = \begin{pmatrix} m^2_{\tilde{L}'} & (A_\nu - \mu\cot\beta)m_D^T & m_D^T M_R \\ (A_\nu - \mu\cot\beta)m_D & m^2_{\tilde{R}} + M_R M_R^T + m_D m_D^T & \pm M_R \mu_S + B_{M_R} \\ M_R^T m_D & \pm\mu_S M_R^T + B_{M_R}^T & m^2_{\tilde{S}} + \mu_S^2 + M_R^T M_R \pm B_{\mu_S} \end{pmatrix}$$

$\Rightarrow$

$$\mathcal{M}^2_{\tilde{\nu}^{\mathcal{I}(\mathcal{R})}} \approx \begin{pmatrix} m^2_{\tilde{L}'} & (A_\nu - \mu\cot\beta)m_D^T & m_D^T M_R \\ (A_\nu - \mu\cot\beta)m_D & m^2_{\tilde{R}} + M_R M_R^T + m_D m_D^T & B_{M_R} \\ M_R^T m_D & B_{M_R}^T & M_R^T M_R \end{pmatrix}$$

In the context of mass eigenstates for d_i and l_i, other fields are rotated to mass eigenstates,

$$\begin{aligned} \mathcal{L}_{\rm LQD} &= \lambda'_{ijk}\big(\tilde{\nu}_{Li}\bar{d}_{Rk}d_{Lj} + \tilde{d}_{Lj}\bar{d}_{Rk}\nu_{Li} + \tilde{d}^*_{Rk}\bar{\nu}^c_{Li}d_{Lj} \\ &- \tilde{l}_{Li}\bar{d}_{Rk}u_{Lj} - \tilde{u}_{Lj}\bar{d}_{Rk}l_{Li} - \tilde{d}^*_{Rk}\bar{l}^c_{Li}u_{Lj}\big) + \text{h.c.} \\ &\Rightarrow \\ \mathcal{L}'_{\rm LQD} &= \lambda'^{\mathcal{I}(\mathcal{R})}_{vjk}\tilde{\nu}_v\bar{d}_{Rk}d_{Lj} + \lambda'^{\mathcal{N}}_{vjk}\big(\tilde{d}_{Lj}\bar{d}_{Rk}\nu_v + \tilde{d}^*_{Rk}\bar{\nu}^c_v d_{Lj}\big) \\ &- \tilde{\lambda}'_{ilk}\big(\tilde{l}_{Li}\bar{d}_{Rk}u_{Ll} + \tilde{u}_{Ll}\bar{d}_{Rk}l_{Li} + \tilde{d}^*_{Rk}\bar{l}^c_{Li}u_{Ll}\big) + \text{h.c.}, \end{aligned}$$

where $\lambda'^{\mathcal{I}(\mathcal{R})}_{vjk} = \lambda'_{ijk}\tilde{\mathcal{V}}^{\mathcal{I}(\mathcal{R})*}_{vi}$, $\lambda'^{\mathcal{N}}_{vjk} = \lambda'_{ijk}\mathcal{V}^*_{vi}$ and $\tilde{\lambda}'_{ilk} = \lambda'_{ijk}K^*_{lj}$

$b \to s\ell^+\ell^-$ process (right-handed currents)

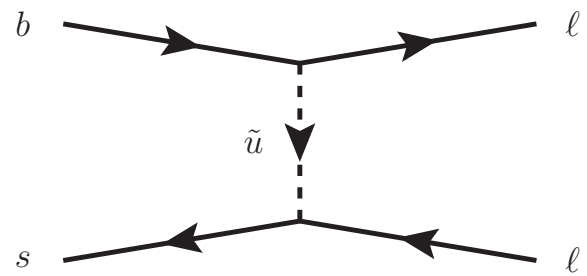

$$C'_{9,\mu} = -C'_{10,\mu} = -\frac{\sqrt{2}\pi^2}{G_F \eta_t e^2} \frac{\tilde{\lambda}'_{2i2}\tilde{\lambda}'^*_{2i3}}{m^2_{\tilde{u}_{Li}}}$$

Besides, for some boxes:

$$C'^{\chi^\pm}_{9,\ell} = -C'^{\chi^\pm}_{10,\ell} = \lambda'^{\mathcal{I}}_{vi2}\lambda'^{\mathcal{I}*}_{v'i3} D_2[m_{\tilde{\nu}^{\mathcal{I}}_v}, m_{\tilde{\nu}^{\mathcal{I}}_{v'}}, m_{\chi^\pm_m}, m_{d_i}](\cdots)$$
$$\cdots$$

Assumption

λ'_{ijk} is non-negligible with the single value k at $\mu_{\rm NP}(= 0.5$ TeV) scale

$b \to s\ell^+\ell^-$ process (box)

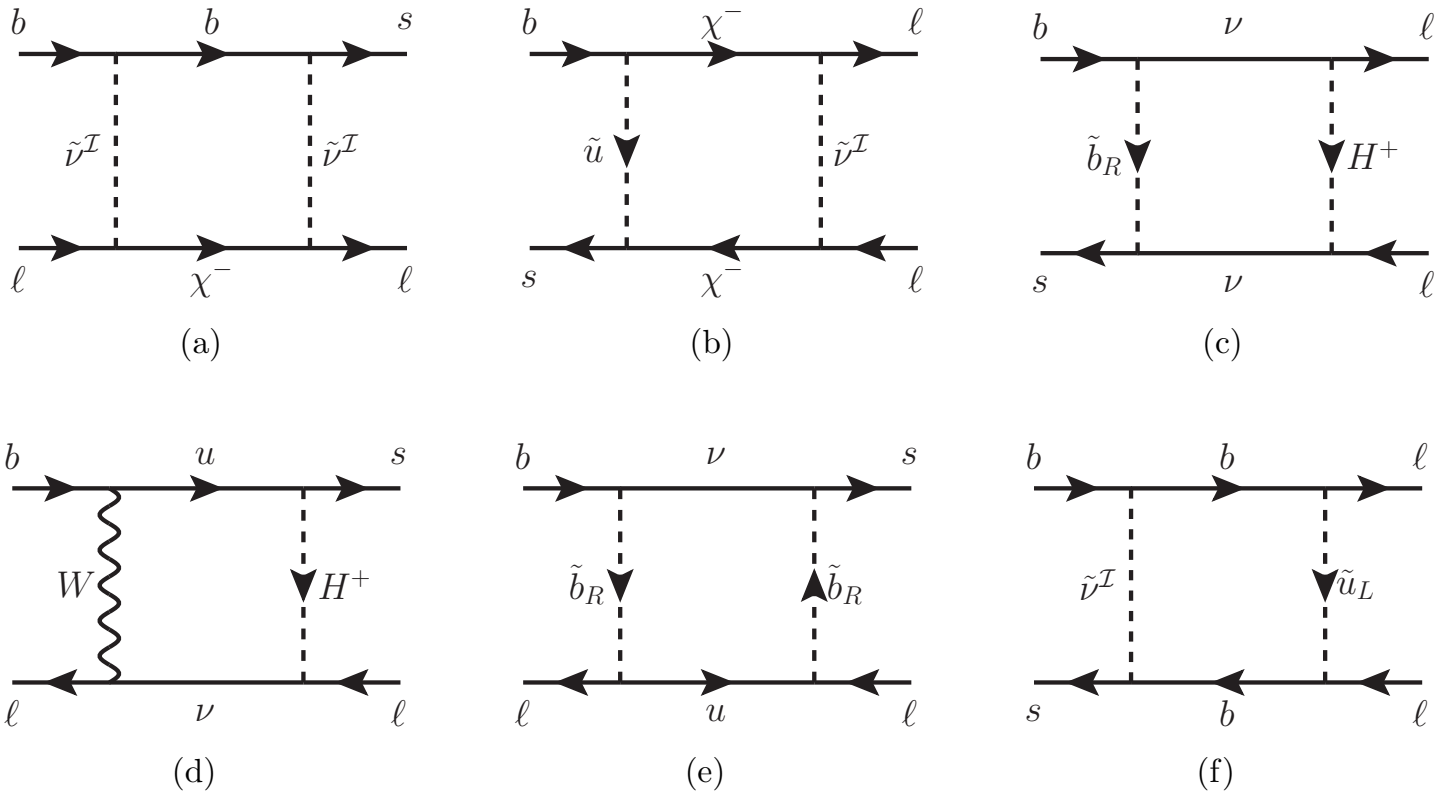

An example of $\chi^{\pm}$ boxes with λ' couplings (a) and without λ' couplings (b), an example of $W(G)/H^{\pm}$ boxes with λ' couplings (c) and without λ' couplings (d), as well as $4\lambda'$ boxes (e, f).

$b \to s\ell^+\ell^-$ process (box)

Under the assumption of sufficiently large $m_{\tilde{b}_R}$, $m_{\tilde{u}_L}$ (~ 10 TeV) and the electron-flavour sector of $\mathcal{M}_{\tilde{\nu}^{\mathcal{I}(\mathcal{R})}}$.

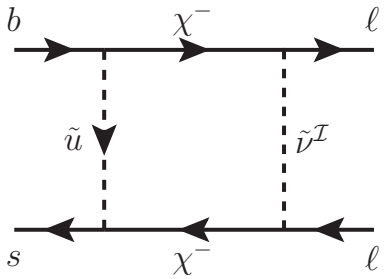

$$C_{\rm V}^{\chi^\pm(1)} = -\frac{\sqrt{2}\pi^2 i}{2G_F\eta_t e^2} y_{u_i}^2 K_{i3}K_{i2}^* V_{m2}^* V_{n2}(g_2 V_{m1}\tilde{\mathcal{V}}^{\mathcal{I}}_{v2} - V_{m2}Y^{\mathcal{I}}_{2v})$$
$$(g_2 V_{n1}^*\tilde{\mathcal{V}}^{\mathcal{I}}_{v2} - V_{n2}^* Y^{\mathcal{I}}_{2v}) D_2[m_{\tilde{\nu}^{\mathcal{I}}_v}, m_{\chi^\pm_m}, m_{\chi^\pm_n}, m_{\tilde{u}_{Ri}}]$$

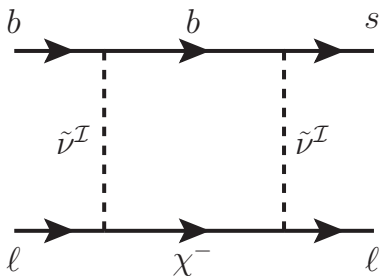

$$C_{\rm V}^{\chi^\pm(2)} = \frac{\sqrt{2}\pi^2 i}{2G_F\eta_t e^2}\lambda'^{\mathcal{I}}_{v3k}\lambda'^{\mathcal{I}*}_{v'2k}(g_2 V_{m1}^*\tilde{\mathcal{V}}^{\mathcal{I}}_{v2} - V_{m2}^* Y^{\mathcal{I}}_{2v})$$
$$(g_2 V_{m1}\tilde{\mathcal{V}}^{\mathcal{I}}_{v'2} - V_{m2}Y^{\mathcal{I}}_{2v'}) D_2[m_{\tilde{\nu}^{\mathcal{I}}_v}, m_{\tilde{\nu}^{\mathcal{I}}_{v'}}, m_{\chi^\pm_m}, m_{d_k}]$$

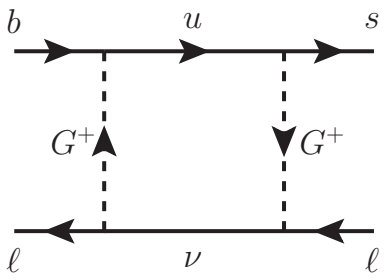

$$\Delta C_{9,\ell}^{G^\pm} = -\Delta C_{10,\ell}^{G^\pm} = \sum_{v_h=4}^{9} -\frac{\sqrt{2}\pi^2 i}{2G_F\eta_t e^2} y_{u_i}^2 K_{i3}K_{i2}^* \sin^4\beta$$
$$|Y_{\nu_{\ell\ell}}\mathcal{V}^T_{(\ell+3)v_h}|^2 D_2[m_{\nu_{v_h}}, m_{u_i}, m_W, m_W]$$

where $Y^{\mathcal{I}}_{\ell v} = (Y_\nu)_{j\ell}\tilde{\mathcal{V}}^{\mathcal{I}*}_{v(j+3)}$

$b \to s\ell^+\ell^-$ process (photon penguin)

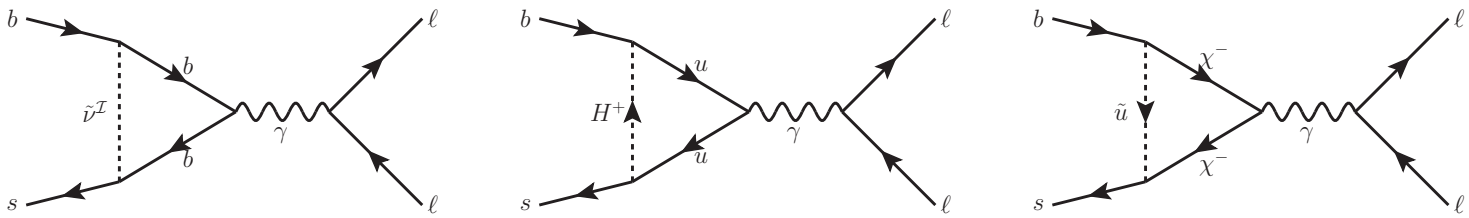

(a) (b) (c)

Each example of the λ' diagrams (left) and the non-λ' diagrams with $W(G)/H^\pm$ (middle) and charginos (right) engaged are shown respectively.

$$\text{Fig.(a)}: \quad C_{\rm U}^{\gamma(1)} = -\frac{\sqrt{2}\lambda'^{\mathcal{I}}_{v33}\lambda'^{\mathcal{I}*}_{v23}}{36 G_F \eta_t m^2_{\tilde{\nu}^{\mathcal{I}}_v}}\left(\frac{4}{3} + \log\frac{m_b^2}{m^2_{\tilde{\nu}^{\mathcal{I}}_v}}\right) \qquad \text{for} \quad k = 3$$

$$C_{\rm V} = C_{\rm V}^{\chi^\pm(1)} + C_{\rm V}^{\chi^\pm(2)} \qquad C_{\rm U} = C_{\rm U}^{\gamma(1)} + C_{\rm U}^{\gamma(2)}$$

$(g-2)_\ell$

$$i\mathcal{M} = ie\bar{\ell}\left(\gamma^\eta + a_\ell \frac{i\sigma^{\eta\beta}q_\beta}{2m_\ell}\right)\ell A_\eta$$

$$\delta a_\ell^{\chi^\pm} = \frac{m_\ell}{16\pi^2}\left[\frac{m_\ell}{6m^2_{\tilde{\nu}_v}}\left(|c_{mv}^{\ell L}|^2 + |c_{mv}^{\ell R}|^2\right)F_1^C(m^2_{\chi_m^\pm}/m^2_{\tilde{\nu}_v}) + \frac{m_{\chi_m^\pm}}{m^2_{\tilde{\nu}_v}}\mathrm{Re}[c_{mv}^{\ell L}c_{mv}^{\ell R}]F_2^C(m^2_{\chi_m^\pm}/m^2_{\tilde{\nu}_v})\right],$$

$$\delta a_\ell^{\chi^0} = \frac{m_\ell}{16\pi^2}\left[-\frac{m_\ell}{6m^2_{\tilde{l}_i}}\left(|n_{ni}^{\ell L}|^2 + |n_{ni}^{\ell R}|^2\right)F_1^N(m^2_{\chi_n^0}/m^2_{\tilde{l}_i}) + \frac{m_{\chi_n^0}}{m^2_{\tilde{l}_i}}\mathrm{Re}[n_{ni}^{\ell L}n_{ni}^{\ell R}]F_2^N(m^2_{\chi_n^0}/m^2_{\tilde{l}_i})\right].$$

where,

$$c_{mv}^{\ell R} = y_\ell U_{m2}\tilde{\mathcal{V}}^{\mathcal{I}}_{v\ell}, \quad c_{mv}^{\ell L} = -g_2 V_{m1}\tilde{\mathcal{V}}^{\mathcal{I}}_{v\ell} + V_{m2}Y^{\mathcal{I}}_{\ell v};$$

$$n_{ni}^{\ell R} = \sqrt{2}g_1 N_{n1}\delta_{i(\ell+3)} + y_\ell N_{n3}\delta_{i\ell}, \quad n_{ni}^{\ell L} = \frac{1}{\sqrt{2}}\left(g_2 N_{n2} + g_1 N_{n1}\right)\delta_{i\ell} - y_\ell N_{n3}\delta_{i(\ell+3)}.$$

$$1.92(1.33) \leqslant |\delta a_\mu^{\chi^\pm} + \delta a_\mu^{\chi^0}| \times 10^9 \leqslant 3.10(3.69)$$

Constraints of related processes

processes	bounds
$K \to \pi\nu\bar{\nu}$	$\lvert\lambda'_{i1k}\rvert \lesssim 10^{-2}$
$\tau \to \mu\rho^0(\phi)$	$\lvert\lambda'_{ij1(2)}\rvert \lesssim 1(1.3)$ (no cancellations)
$B \to X_s\gamma$	$\lvert C_7^{\rm NP}\rvert < 0.025$
$B_s - \bar{B}_s$ mixing	$0.90 < \lvert 1 + C_{B_s}^{\rm NP}/C_{B_s}^{\rm SM}\rvert < 1.11$

Under the premise of no flavour mixing in $\tilde{\mathcal{V}}^{\mathcal{I}(\mathcal{R})}$ while chiral mixings remain:

- For satisfying the bounds from charged lepton flavour violating decays
- sufficiently heavy $m_{\tilde{L}'_1}$ and $m_{\tilde{R}_1}$ can eliminate $b \to se^+e^-$ boxes except for $\Delta C^{G^\pm}_{9(10),e}$
- $m_{\tilde{\mu}_R}$ and $m_{\tilde{L}'_1}$ are set sufficiently heavy for non-dominant $|\delta a_\mu^{\chi^0}|$ and $|\delta a_e^{\chi^\pm}|$

Constraints and prospects: anomalous $t \to cV(h)$ decays

$\mathcal{B}(t \to cZ)_{\rm LHC} < 2.4 \times 10^{-4}$ (ATLAS, M. Aaboud *et al.*, JHEP 07 (2018) 176)

$\mathcal{B}(t \to c\gamma)_{\rm LHC} < 1.8 \times 10^{-4}$ (ATLAS, G. Aad *et al.*, PLB 800 (2020) 135082)

$\mathcal{B}(t \to cg)_{\rm LHC} < 4.1 \times 10^{-4}$ (CMS, V. Khachatryan *et al.*, JHEP 02 (2017) 028)

$\mathcal{B}(t \to ch)_{\rm LHC} < 1.1 \times 10^{-3}$ (ATLAS, M. Aaboud *et al.*, JHEP 05 (2019) 123)

$$V^{\mu}(tcg) = ig_s t^a \left(ik_\nu \sigma^{\mu\nu} P_R B^g\right),$$

$$B^g = -\frac{\tilde{\lambda}'^{*}_{i2k}\tilde{\lambda}'_{i3k}}{16\pi^2} m_t [c_{11} - c_{12} + c_{21} - c_{23}](-p_t, p_c, m_{d_k}, m_{\tilde{l}_{Li}}, m_{d_k}),$$

$$\Gamma^{\rm NP}(t \to cg) = \frac{g_s^2 m_t^3}{12\pi} |B^g|^2.$$

$\tilde{\lambda}'^{*}_{i2k}\tilde{\lambda}'_{i3k} f(\tilde{l}_{Li}) \approx (\lambda'^{*}_{i2k}\lambda'_{i3k} + |\lambda'_{i2k}|^2 K_{cb} + |\lambda'_{i3k}|^2 K_{cb}) f(\tilde{l}_{Li})$

Choice of input parameters

Parameters	Sets	Parameters	Sets
$\tan\beta$	15	Y_ν	$\mathrm{diag}(0.7, 0.8, 0.5)$
M_1	320 GeV	M_R	$\mathrm{diag}(1, 1, 1)$ TeV
M_2	350 GeV	B_{M_R}	$\mathrm{diag}(0.5, 0.5, 0.5)$ TeV^2
μ	450 GeV	A_ν	$0/\mathrm{diag}(0, -1.5, 0)$ TeV
$m_{\tilde{u}_{Ri}}$	1.5 TeV	$m_{\tilde{L}'_1}$	5 TeV
$m_{\tilde{\mu}_R}$	5 TeV	$m_{\tilde{R}}$	$\mathrm{diag}(5, 0, 0)$ TeV

provide $m_{\chi_1^\pm} = 325$ GeV, $m_{\chi_1^0} = 307$ GeV

ATLAS, G. Aad *et al.*, EPJC 80 (2020) 2, 123

ATLAS, G. Aad *et al.*, PRD 101 (2020) 5, 052005

$\sin^2\theta_{12}$	$\sin^2\theta_{23}$	$\sin^2\theta_{13}$
$0.304(12)$	$0.573^{+0.016}_{-0.020}$	$0.02219^{+0.00062}_{-0.00063}$
$\delta_{CP}[^\circ]$	$\Delta m^2_{21}[10^{-5}\ \mathrm{eV}^2]$	$\Delta m^2_{31}[10^{-3}\ \mathrm{eV}^2]$
197^{+27}_{-24}	$7.42^{+0.21}_{-0.20}$	$2.517^{+0.026}_{-0.028}$

$m_\nu^{\mathrm{diag}} \approx \mathrm{diag}(0, \sqrt{\Delta m^2_{21}}, \sqrt{\Delta m^2_{31}}) = \mathrm{diag}(0, 0.008, 0.05)$ eV

I. Esteban *et al.*, JHEP 09 (2020) 178

$(g-2)_\mu$

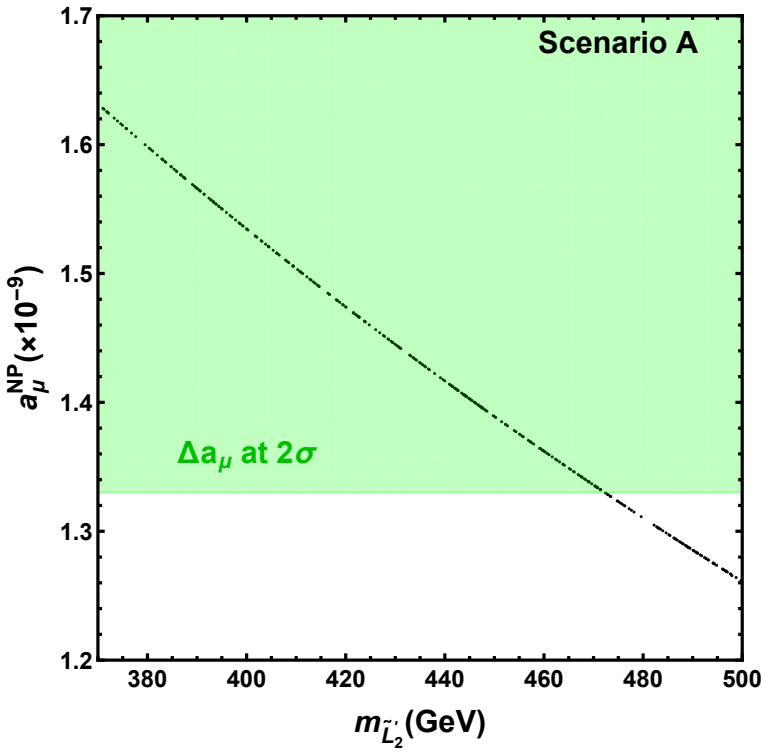

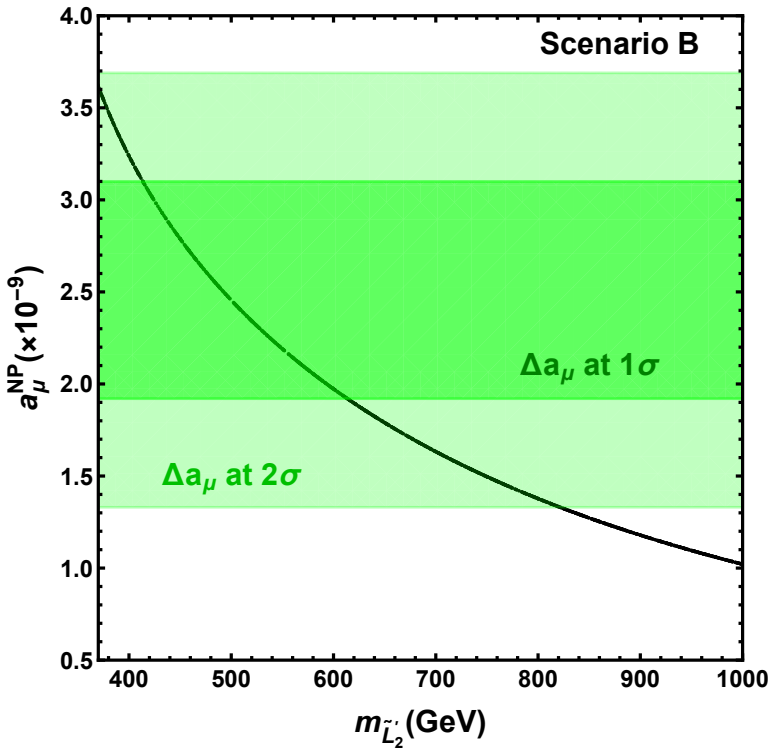

Left: scenario A, right: scenario B.

Scenario A

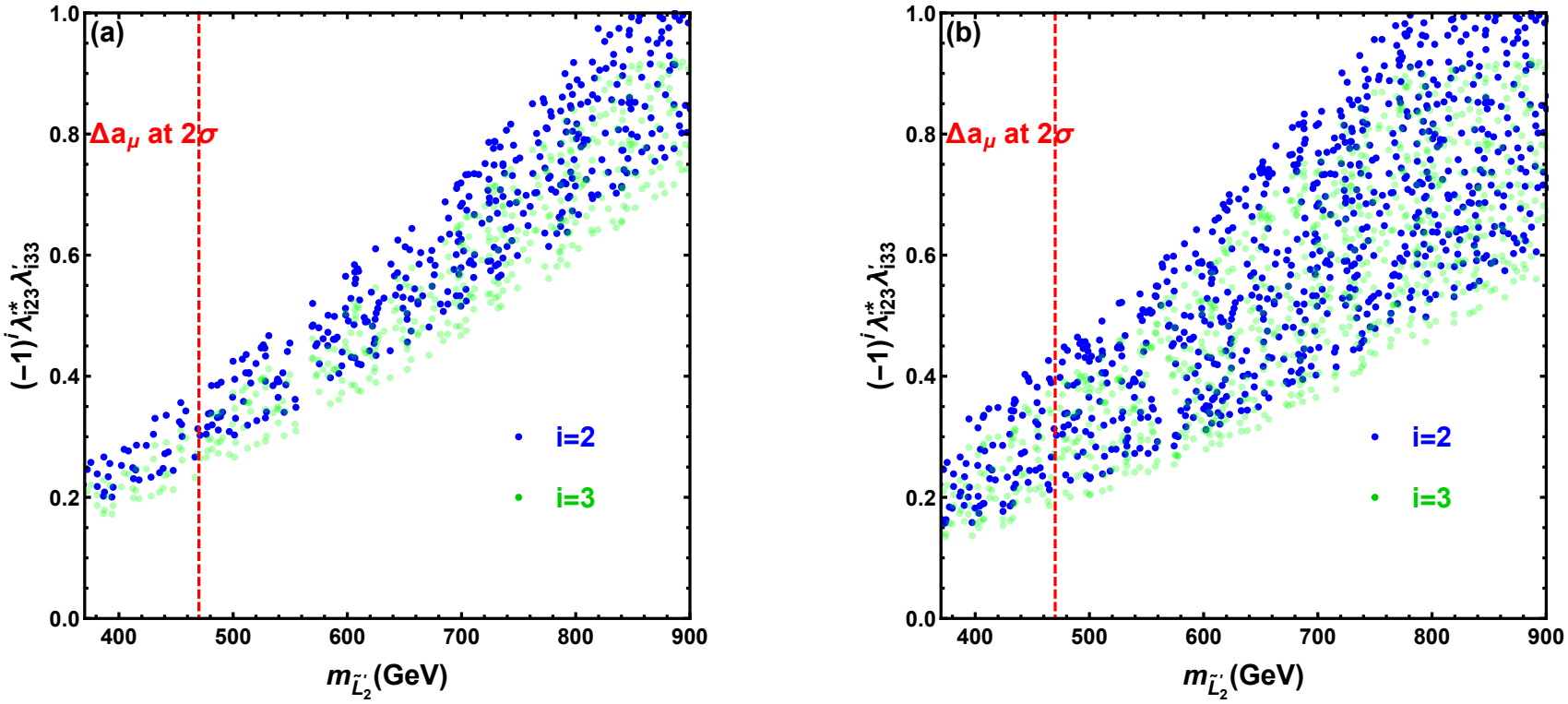

Blue(green) points denote $\lambda'^*_{223}\lambda'_{233}$ $(-\lambda'^*_{323}\lambda'_{333})$ varies with $m_{\tilde{L}'_2}$, and $\lambda'^*_{323}\lambda'_{333}$ $(\lambda'^*_{223}\lambda'_{233})$ is fixed with $C_{\rm U} = 0$. (a): 1σ fit, (b): 2σ fit.

Scenario B

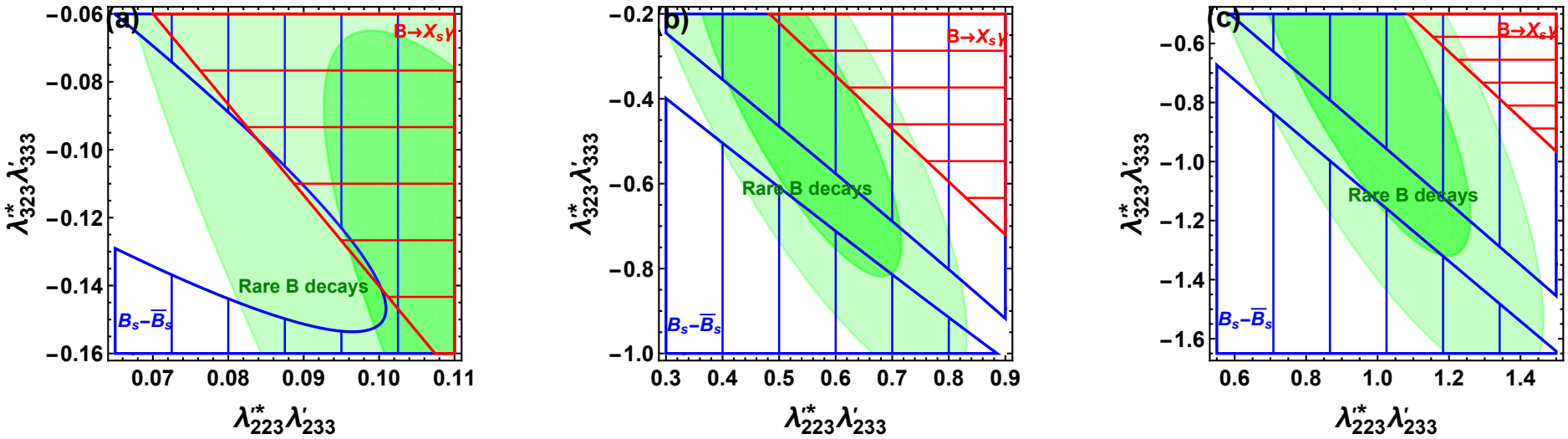

The green regions are $1(2)\sigma$ favored ones with dark (light) opacity to satisfy the rare B-meson decay fits. $m_{\tilde{L}'_3} = m_{\tilde{L}'_2}$ is fixed as 430 (left), 750 (middle) and 1000 GeV (right).

Scenario B

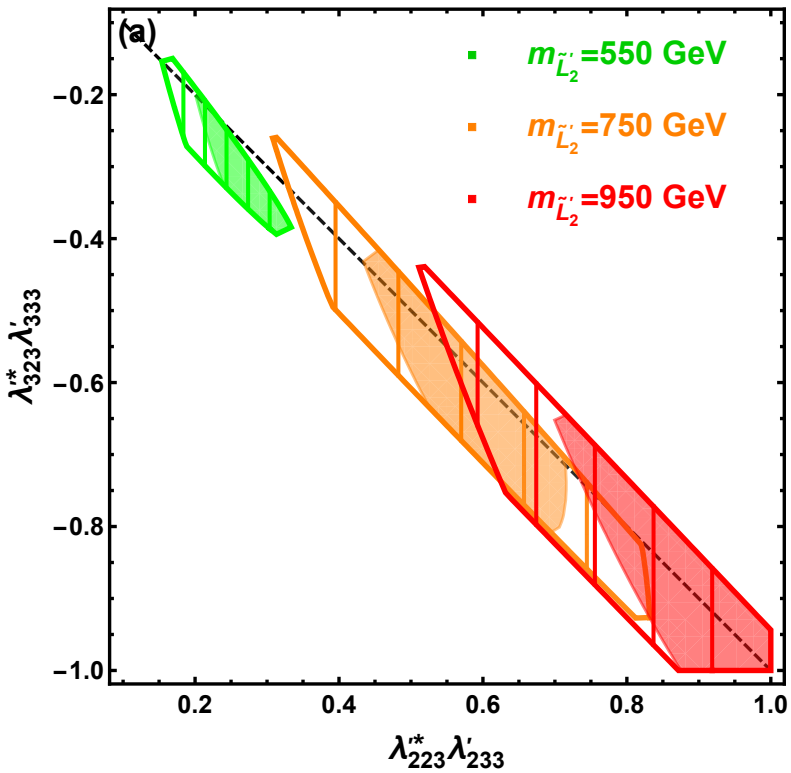

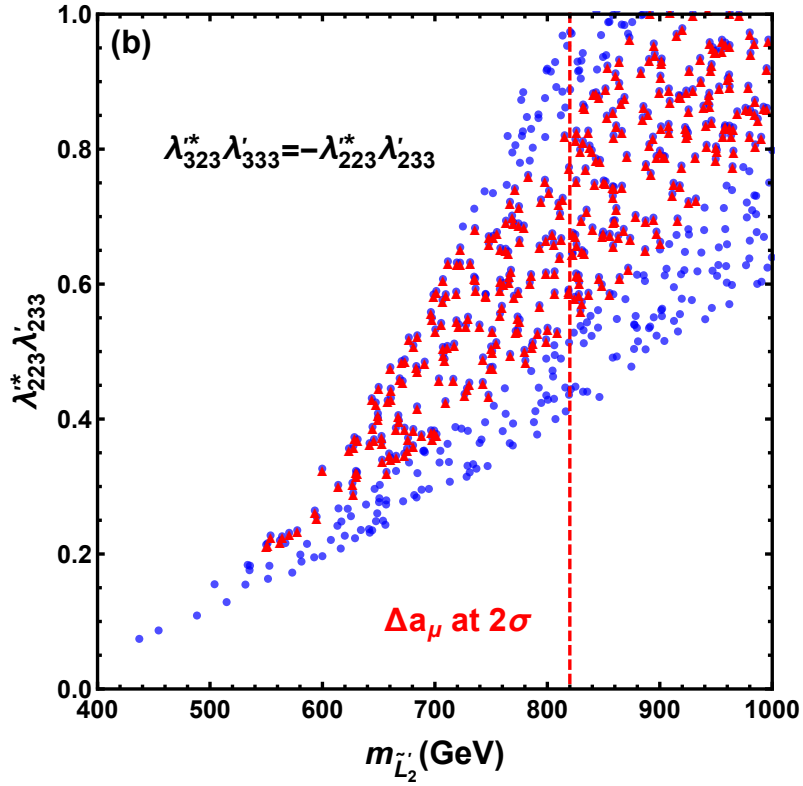

(a): $m_{\tilde{L}_3'} = m_{\tilde{L}_2'} = 550$ (green), 750(orange) and 950 GeV (red) at 1σ (painted areas) and 2σ (hatched areas) levels of the rare B-meson decay fits.
(b): Assuming $\lambda'^*_{323}\lambda'_{333} = -\lambda'^*_{223}\lambda'_{233}$. Red (blue) points denote the rare B-meson decay fit at $1(2)\sigma$ level.

Final common regions to explain the two anomalies

Scenario A:

$m_{\tilde{L}'_2}$ [GeV]	$\lambda'^*_{223}\lambda'_{233}$	$\lambda'^*_{323}\lambda'_{333}$
370	$[0.14, 0.30]$	$[-0.26, -0.12]$
420	$[0.17, 0.37]$	$[-0.32, -0.15]$
470	$[0.20, 0.44]$	$[-0.38, -0.18]$

Scenario B:

$m_{\tilde{L}'_2}$ [GeV]	$\lambda'^*_{223}\lambda'_{233}$	$\lambda'^*_{323}\lambda'_{333}$
420	$[0.062, 0.086]$	$[-0.137, -0.063]$
650	$[0.22, 0.62]$	$[-0.70, -0.17]$
820	$[0.35, 1.00]$	$[-1.10, -0.30]$

Predictions of $\mathcal{B}(t \to cg)_{\rm NP}$

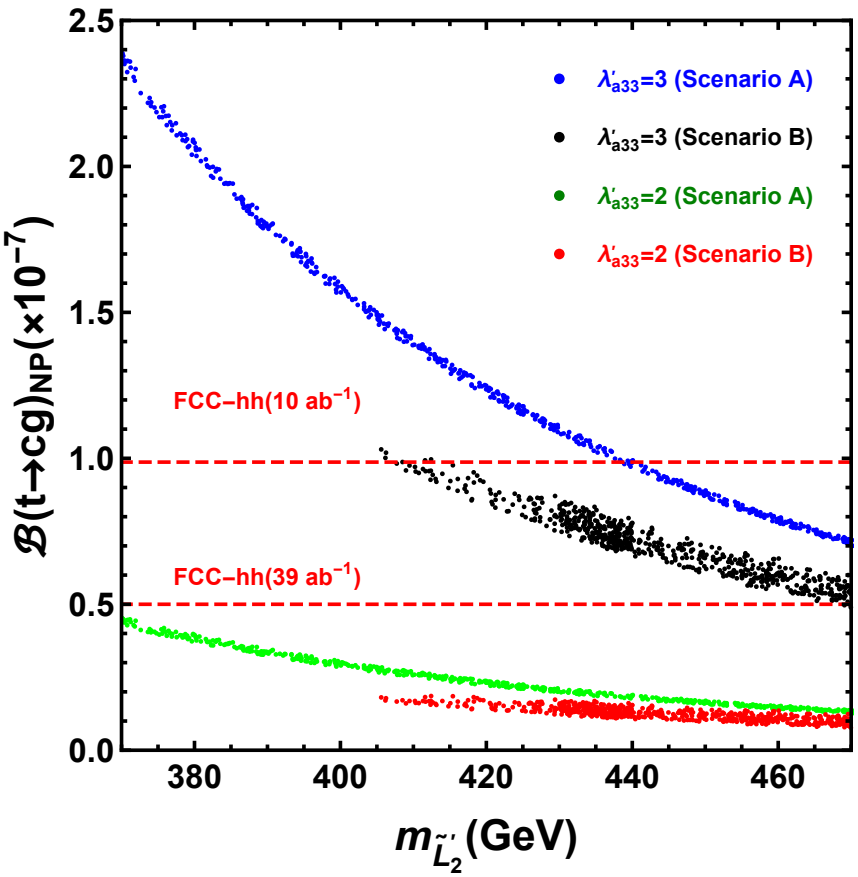

The predictions of $\mathcal{B}(t \to cg)_{\rm NP}$ compared with the prospect upper limit at 100 TeV FCC-hh. $\mathcal{B}(t \to cg)_{\text{FCC-hh}} = 9.87 \times 10^{-8}$ for $\mathcal{L} = 10$ ab^{-1} through the triple-top signal.
H. Khanpour, NPB 958 (2020) 115141

At FCC-hh, this model signal on the $t \to cg$ transition has considerable possibilities to be found for sufficiently large λ'_{a33} (e.g., $\lambda'_{233} = \lambda'_{333} = 3$).

Conclusions

- We scrutinize all the one-loop contributions to $b \to s\ell^+\ell^-$ processes under the assumption of a single value k in RPV-MSSMIS. Among them, the contributions of chiral mixing between LH and singlet (s)neutrinos within superpotential term $\lambda'_{ijk}\hat{L}_i\hat{Q}_j\hat{D}_k$ are given for the first time to our knowledge.

- We find that $b \to s\ell^+\ell^-$ and $(g-2)_\mu$ anomalies can be explained simultaneously in both scenarios of model-independent global fits. Also, we make a prospect that NP contributions to $t \to cg$ process can reach the sensitivity at FCC-hh in parts of the parameter spaces of this model.

Backup

$$\mathcal{V}^T \approx \begin{pmatrix} 0.840 & 0.509 & -0.147 & -0.085i & 0 & 0 & 0.085 & 0 & 0 \\ -0.231 & 0.599 & 0.755 & 0 & 0.097i & 0 & 0 & 0.097 & 0 \\ 0.478 & -0.608 & 0.628 & 0 & 0 & 0.061i & 0 & 0 & -0.061 \\ 0 & 0 & 0 & 0.707i & 0 & 0 & 0.707 & 0 & 0 \\ 0 & 0 & 0 & 0 & -0.707i & 0 & 0 & 0.707 & 0 \\ 0 & 0 & 0 & 0 & 0 & -0.707i & 0 & 0 & -0.707 \\ -0.102 & -0.062 & 0.018 & -0.702i & 0 & 0 & 0.702 & 0 & 0 \\ 0.032 & -0.083 & -0.105 & 0 & 0.700i & 0 & 0 & 0.700 & 0 \\ -0.041 & 0.053 & -0.055 & 0 & 0 & 0.704i & 0 & 0 & -0.704 \end{pmatrix}$$